N O T I C E

THIS DOCUMENT HAS BEEN REPRODUCED FROM MICROFICHE. ALTHOUGH IT IS RECOGNIZED THAT CERTAIN PORTIONS ARE ILLEGIBLE, IT IS BEING RELEASED IN THE INTEREST OF MAKING AVAILABLE AS MUCH INFORMATION AS POSSIBLE

NASA

Technical Memorandum 82026

Pulsar Gamma-Rays: Spectra, Luminosities and Efficiencies

Alice K. Harding

SEPTEMBER 1980

National Aeronautics and
Space Administration

Goddard Space Flight Center
Greenbelt, Maryland 20771

PULSAR γ-RAYS: SPECTRA, LUMINOSITIES AND EFFICIENCIES

Alice K. Harding

Laboratory for High Energy Astrophysics

NASA/Goddard Space Flight Center

Greenbelt, MD 20771

ABSTRACT

The general characteristics of pulsar γ-ray spectra are presented for a model where the γ-rays are produced by curvature radiation from energetic particles above the polar cap and attenuated by pair production. The shape of the spectrum is found to depend on pulsar period, magnetic field strength, and primary particle energy. By a comparison of numerically calculated spectra with the observed spectra of the Crab and Vela pulsars, it is determined that primary particles must be accelerated to energies of $\sim 3\times10^{7}$ mc^{2}. A general formula for pulsar γ-ray luminosity is determined and is found to depend on period and field strength. The γ-ray efficiency scales with characteristic age as $\tau^{1.8}$ up to $\tau \sim 3\text{-}4\times10^{7}$ yr., where there may be a turnoff in the γ-ray emission.

I. INTRODUCTION

High energy pulsed γ-ray emission from the two shortest period radio pulsars is now well established observationally. The Crab and Vela pulsars have been studied extensively in the last few years by SAS2 (Kniffen et al. 1974, Thompson et al. 1975) and by COSB (Bennett et al. 1977) at energies above 30 MeV. The γ-ray emission from these pulsars is a much higher fraction of the total energy loss rate than the radio emission and, therefore, must play a major role in the radiation mechanism. The energy spectra of the Crab and Vela have recently been reanalyzed in the range 50 MeV-2 GeV from COSB data (Lichti et al. 1980), and they fit steep power laws with slopes of -2.17 and -1.89.[1]

Although only a small fraction of the 328 known radio pulsars have been detected in the γ-ray range, it is possible that many of these pulsars are emitting pulsed γ-rays below the present detectability limits. If γ-ray emission is a general characteristic, an important question is whether the production mechanism is the same for all pulsars. The similar pulse shapes and spectra of the Crab and Vela argue strongly in favor of a single mechanism for these two pulsars, though their properties are quite different at other energies. From a theoretical point of view, it is essential to try to establish the characteristics of pulsar γ-ray emission in specific models for the whole range of pulsar parameters such as period and magnetic field strength. When γ-ray data on other pulsars becomes available from more sensitive detectors, it may then be possible to use these characteristics as a test of certain models for γ-ray pulsars as a class.

---

[1] Detection of pulsed emission from PSR1747-46 has also been reported (Ögelman et al. 1976, Thompson et al. 1976), but this result is now in question because of a recent radio timing observation (Newton et al. 1980) which measured a much lower period derivative than was used to determine the γ-ray light curve.

It is the purpose of this paper to outline some observable characteristics of pulsar γ-ray emission in a particular model and to determine a general luminosity formula which is a function of pulsar parameters. This model assumes that the γ-ray emission above 100 MeV is produced by primary particles undergoing curvature radiation in the magnetic field above the pulsar polar cap. These particles have been accelerated along field lines by the intense electric fields induced by rotation. Because of the extremely high energies to which the particles are accelerated (Sturrock 1971; Ruderman and Sutherland 1975; Scharlemann, Arons and Fawley 1978), their curvature radiation spectrum extends well into the γ-ray range. The most important attenuation mechanism affecting these γ-rays is magnetic field induced pair production, which becomes important around 500 MeV.

The details of this model were presented in an earlier paper (Harding, Tademaru and Esposito 1978, hereafter referred to as Paper I), in which the γ-rays were traced from their emission points through the rotating magnetosphere and attenuated by pair production. Optical depths, pulse shapes, and spectra were calculated in the case where the emitting primary particles are monoenergetic. It was found that pulsar rotation increases the amount of pair production, primarily through the induced electric field perpendicular to the magnetic field. The electric field increases the pair production rate above the value it would have in a pure magnetic field (Daugherty and Lerche 1975). As a result, high energy γ-rays are more severely attenuated in short period pulsars. Salvati and Massaro (1978) obtained similar results using the same type of model, but including some synchrotron radiation from secondary pairs.

This paper assumes a monoenergetic injection spectrum of primaries and takes into account the energy loss of the particles as they radiate (§ II). This produces steeper γ-ray spectra than those calculated in Paper I for constant primary particle energy. Numerically calculated spectra for various pulsar parameters and primary particle energies are presented in § III and are compared to the COSB spectra of the Crab and Vela. In § IV, the dependence of γ-ray luminosity on period and magnetic field strength is derived from the integrated spectra. A prediction of the dependence of efficiency on characteristic age is also discussed.

II. CURVATURE RADIATION SPECTRUM

Paper I describes the basic assumptions and approximations of the model and also the numerical technique used to calculate the pair production rate as the photons move out from their emission points. The emission spectrum here differs from that described in Paper I in that it allows for energy loss by the emitting particles as they move out from the accelerating region. The calculation does not deal with the specifics of the acceleration mechanism but rather assumes that the particles somehow reach highly relativistic energies near the star.

Several methods of particle acceleration above the polar cap have been discussed (Ruderman and Sutherland 1975; Scharlemann Arons and Fawley 1978; Arons and Scharlemann 1979) as well as acceleration in the outer magnetosphere (Cheng, Ruderman, and Sutherland 1976). These studies determine the energy, γ_o, to which the particles are accelerated as a function of

period P, magnetic field strength B_o, and radius of curvature, R_c, of the field lines. It is found that, while very large electric fields can be induced along the B field lines, acceleration is basically limited by pair production discharges which short out the E field. As a result of these competing processes each of which depend on P and B_o, the net potential drop has only a weak dependence on these parameters. In this calculation, we will simply assume that γ_o does not depend either on P or B_o.

We assume that a monoenergetic beam of primary particles of energy γ_o is injected uniformly over the polar cap and moves out along dipole field lines. As the particles radiate, they will be losing energy at a rate,

$$\left(\frac{d\gamma}{dt}\right)_{curv.} = \frac{2}{3}\frac{e^2}{mc^3}\left(\frac{c}{R_c}\right)^2 \gamma^4 \qquad (1)$$

where $R_c \simeq \frac{4}{3}\frac{r}{\theta}$ is the magnetic field line radius of curvature for a dipole field. The equilibrium distribution of particles at (r,θ) will be,

$$N(\gamma,r,\theta) = \frac{N_o\,(c/R_c)}{(d\gamma/dt)_{curv}}\left(\frac{r_o}{r}\right)^3, \qquad \gamma \le \gamma_{max}\,(r,\theta) \qquad (2)$$

where $\gamma_{max}\,(r,\theta)$ is the maximum particle energy at (r,θ), obtained by integrating the expression for $(d\gamma/dt)_{curv}$ along a field line:

$$\gamma_{max}\,(r,\theta) = \gamma_o\,[3.16\times 10^{-13}\,\frac{\theta^2}{r}\ln\left(\frac{r}{r_o}\right)\gamma_o^3 + 1]^{-1/3} \qquad (3)$$

N_o is the density of primary particles at the stellar surface, r_o, emerging from the acceleration zone. Since we are ignoring the details of the acceleration, we simply assume that N_o is proportional to the corotation charge density:

$$N_o = \frac{n\rho_c}{e} = \frac{n\Omega B}{2\pi ec} = 7\times10^{10}\ n\ P^{-1}\ B_{12}\ cm^{-3} \tag{4}$$

where B_{12} is the surface magnetic field in units of 10^{12} gauss. The emission coefficient at point (r,θ) will therefore be

$$\varepsilon(\omega, r, \theta) = \int_{\gamma_{max}(r,\theta)}^{\gamma_f} N(\gamma, r, \theta)\ P(\omega)\ d\gamma \tag{5}$$

where

$$P(\omega) = \frac{\sqrt{3}}{2\pi}\ \frac{e^2}{c}\ \frac{c}{R_c}\ \gamma\ (\frac{\omega}{\omega_c}) \int_{\frac{\omega}{\omega_c}}^{\infty} K_{5/3}(x)\ dx$$

$$\approx \sqrt{\frac{3}{\pi}}\ \frac{e^2}{c}\ \omega^{1/3}\ \Gamma\ (\frac{2}{3})\ (\frac{c}{R_c})^{2/3},\ \omega \le \omega_c$$

$$\omega_c = \frac{3}{2}\ \gamma^3\ \frac{c}{R_c} \tag{6}$$

(Jackson 1962) is the instantaneous power emitted per electron and ω_c is the critical frequency, above which the spectrum cuts off. The upper integration limit in equation (5), γ_f, is the lowest particle energy which can produce photons of frequency ω, or

$$\gamma_f(\omega) = \left[\frac{2}{3}\frac{R_c}{c}\omega\right]^{1/3}$$

Performing the integration in equation (5), we find,

$$\epsilon(\omega, r, \theta) = \frac{3^{7/6}}{4} \pi^{-\frac{1}{2}} N_o mc^2 \left(\frac{R_c}{c}\right)^{1/3} \left(\frac{r_o}{r}\right)^3 \omega^{1/3} \left[\frac{1}{2} \frac{c}{R_c} \omega^{-1} - \frac{1}{3} \frac{1}{\gamma^3_{max}}\right] \text{erg s}^{-1} \text{Hz}^{-1} \text{cm}^{-3} \tag{7}$$

This is the energy spectrum radiated by primary particles in a volume element of the magnetosphere. The radiation will be highly beamed in a direction tangent to the field lines, and emission points are chosen so that photons in a given part of the pulse arrive at a stationary observer simultaneously. The determination of emission points and the subsequent attenuation of the radiation by pair production has been detailed in Paper I. Since the secondary pairs are produced at an angle to the field, they will lose most of their energy by synchrotron radiation. While this radiation may contribute to the γ-ray spectrum, the contribution above 100 MeV will come from the high energy tail of the steep primary spectrum. We assume that this is a small effect, though it has not been fully determined, and neglect the radiation from secondary particles in the present calculation.

III. CALCULATED SPECTRA

Spectral points are calculated in this model by integrating the intensity at a given photon energy across the pulse profile. The free parameters determining the shape and magnitude of the spectrum are the period P, the surface magnetic field strength B_o, the initial primary particle energy γ_o,

and number density n. The angle between the magnetic field and spin axes is taken to be 90^{o} in all calculations, with the observer's line of sight passing through the magnetic pole.

For given values of P and B_o, γ_o uniquely determines the shape of the spectrum and n determines the normalization. Figures 1, 2, and 3 show calculated spectra for n = 1 and various values of B_o, γ_o and P. The value of γ_o clearly has a large effect on the curvature radiation cutoff which is in part responsible for the turnover in the spectrum at high energies. Pair production also steepens the high energy part of the spectrum and depends on both P and B_o. The effect of P can be seen by comparing the shapes of the spectra shown in each Figure, which are calculated for the same values of B_o and γ_o. The spectra steepen at lower energies for shorter period pulsars as a result of the higher pair production rates caused by rotation. Increasing B_o also increases pair production and, therefore, also has a steepening effect on the spectrum. The spectra for P = .089 s. in Figures 1 and 2 are nearly identical in shape to the spectra obtained by Salvati and Massaro (1978) in their Figures 4a and 4b for $B_o = 10^{12}$ gauss. Since they have included a contribution from secondary pairs and our calculations have not, it appears that the secondary pairs do not contribute significantly to the spectrum above 100 MeV.

If a value $B_o = 10^{12}$ gauss is assumed, then the best fit spectrum to the COSB data points for the Crab with P = .033 s. is the one having $\gamma_o = 3 \times 10^{7}$ and requires that $n = 1.2 \times 10^{3}$ for normalization at 100 MeV (assuming a distance of 2 kpc.) A lower value of γ_o will fall below the high energy points. These same values for γ_o, n and B_o, but with P = .089 s, also fit the spectral points for Vela quite well (assuming a distance of 0.5 kpc.) These spectra and their fits to the data are shown in Figure 4. The fact that both the Crab and Vela spectra can be fit with the same value of γ_o

strongly supports the prediction of acceleration theories that the particle energy depends only weakly, if at all, on the pulsar period. It also indicates that, in order to account for the highest energy γ-radiation from these pulsars, the acceleration mechanism must be capable of producing particles with $\gamma_o \geq 3 \times 10^7$, and particle densities $n \sim 10^3$ times the corotation charge density. Energies this high are not acheived in the present models for acceleration above the polar cap where potentials only reach $\sim 10^{12}$ volts, though particle densities of this magnitude are. Possibly, the highest energy particles are accelerated, or reaccelerated, in outer gaps where potentials can reach $\sim 10^{14}$ volts (Cheng, Ruderman and Sutherland 1976). As we have found in Paper I, high energy photons which are observed must actually be produced further out in the magnetosphere where the optical depths are lower, and the field line curvature is greater.

IV. γ-RAY LUMINOSITY

The calculated spectra have been integrated for a range of pulsar periods and magnetic field strengths to obtain the dependence of γ-ray luminosity on these parameters. A fit to the numerically integrated spectra gives an expression for the luminosity above 100 MeV, normalized to the Crab with L_γ (> 100 MeV) = 1.4×10^{38} photon s^{-1} and $B_{12} = 3.8$,

$$L_\gamma \text{ (> 100 MeV)} = 1.2 \times 10^{35} B_{12}^{.95} P^{-1.7} \text{ photons } s^{-1} \qquad (8)$$

where B_{12} is in units of 10^{12} gauss. This formula gives L_γ (> 100 MeV) = 2.3×10^{37} s^{-1} for the parameters of Vela ($B_{12} = 3.4$, P = .089 s), which is in good agreement with the observed value 2.4×10^{37} s^{-1} (Lichti et al. 1980).

Without considering the attenuation due to pair production, one would expect in this type of model that

$$L_\gamma \propto \gamma_o N_o \pi r_p^2 c, \tag{9}$$

where r_p is the polar cap radius. If γ_o is independent of P and B_o, as we have assumed, $N_o \propto B_o P^{-1}$, and $r_p = r_o (\Omega r_o/c)^{\frac{1}{2}} \propto P^{-\frac{1}{2}}$, then $L_\gamma \propto B_o P^{-2}$. The departures from this dependence in equation (8) therefore result from the inclusion of pair production attenuation. Since pair production is greater in shorter period pulsars, their luminosities are decreased relative to longer period pulsars.

Luminosities and fluxes for other pulsars can be predicted from equation (8). The magnetic field strength is usually estimated from the amount of radiation reaction torque implied by the value of the period derivative, $\dot{P}$ (Ostriker and Gunn 1969)

$$B_o \simeq 3.2 \times 10^{19} \left(\frac{I/r_o^6}{10^9 \text{ g cm}^{-4}}\right)^{\frac{1}{2}} (P \dot{P})^{\frac{1}{2}} \text{ gauss}. \tag{10}$$

While it is reasonable to assume that all neutron stars have comparable masses, and therefore similar moments of inertia, I, and radii, r_o, it is also possible that the range of observed $P\dot{P}$ indicates a range of neutron star masses. In other words, it is possible that the value of B_o is the same for all pulsars. However, observational determinations of the masses of neutron stars in orbit around binary companions (Rappaport and Joss 1979, Taylor et. al. 1979) have all been consistent with $1.4 \pm 0.2\ M_\odot$, which seems

to suggest a very small mass range. The observed values of $P\dot{P}$ also give a reasonable range for B_o (2×10^{10} - 2×10^{13} gauss) if a constant value of I/r_o^6 is assumed.

For pulsars with measured values of $\dot{P}$, the estimates of B_o, assuming canonical values of $I = 10^{45}$ g cm^2 and $r_o = 10^6$ cm, are used in deriving the luminosity. For all other pulsars, a value of $B_o = 10^{12}$ gauss is assumed. The pulsars with the highest predicted γ-ray fluxes are listed in Table 1 with their luminosities and other measured parameters from Manchester and Taylor (1980). Most of these have fluxes well below those of the Crab (PSR 0531 + 21) and Vela (PSR 0833-45), but a few have comparable predicted fluxes. Eight are above the point source detectability limit of COSB, but all are either outside the latitude range of the search or near the galactic center where the diffuse background is high. All of the pulsars in Table 1 with previously reported period derivatives have been searched for pulsed γ-ray emission by SAS2 and COSB. The predicted fluxes for PSR 0950 + 08, PSR 1642-03, PSR 1706-16 and PSR 1929 + 10 exceed the flux upper limits reported by SAS2 (Ogelman et al. 1976), but by no more than a factor of 3. This is not a serious discrepancy, considering that the errors in the SAS2 limits are of the same magnitude.

Pulsar γ-ray efficiency is defined as the fraction of the total energy loss rate which is radiated in γ-rays. From equation (8) and the expression for the rotational energy loss rate,

$$\frac{dE}{dt} = 4\pi^2 I \frac{\dot{P}}{P^3} \text{ erg s}^{-1}, \tag{11}$$

the efficiency above 100 MeV will be

$$\eta_\gamma = \frac{L_\gamma (> 100 \text{ MeV})}{dE/dt} = \frac{2.0 \times 10^{31}}{4\pi^2 I} B_{12}^{.95} \frac{P^{1.3}}{\dot{P}}. \tag{12}$$

For constant moment of inertia, the efficiency can be expressed in terms of the pulsar's characteristic age, $\tau = \frac{1}{2}(P/\dot{P})^{\frac{1}{2}}$, using equation (10):

$$\eta_\gamma = 4\times10^{-14}\ \dot{P}^{1.3}\tau^{1.8} \qquad (13)$$

where $\dot{P}$ is in units of 10^{-15} s s^{-1} and τ is in years. For the two pulsars with measured γ-ray luminosities, there seems to be an increase in efficiency with age. Figure 5 shows that the quantity $\eta_\gamma\ \dot{P}^{-1.3}$ plotted against τ for these pulsars is consistent with a $\tau^{1.8}$ dependence. Equation (13) predicts that η_γ will exceed 1 above some characteristic age which is equal to $\sim 3\times10^7$ years for $\dot{P} \sim 10^{-15}$ s s^{-1}. This suggests that the γ-ray emission mechanism may turn off before this point since the efficiency cannot exceed 1. One explanation for a γ-ray turnoff is that the primary particle energy, which was assumed to be constant in deriving equation (13), begins decreasing with increasing P at the point where the induced electric fields are no longer shorted out by pair production. Beyond this point, the acceleration grows weaker, producing fewer and lower energy γ-rays, which also cannot produce the particle-photon cascades necessary for the radio emission. The fact that there are few radio pulsars (with measured values of $\dot{P}$) which have characteristic ages greater than $\sim 3\times10^7$ years implies that the radio emission also turns off around this value of τ and may be the result of a γ-ray turnoff.

These results on pulsar γ-ray efficiency roughly agree with the estimate of Buccheri et al. (1978) that $\eta_\gamma \propto \tau$. They also have estimated γ-ray fluxes for 88 pulsars with measured values of $\dot{P}$ and listed those considered to be potentially observable. All of the pulsars in Table 1 do not appear in the list of Buccheri et al. because many did not have measured values of $\dot{P}$ at the time. They also chose a lower limit to the flux detectability of the COSB satellite of 0.1 times the Crab flux and therefore included some pulsars with lower predicted fluxes which do not appear in our list.

V. DISCUSSION

This paper has investigated the dependence of pulsar γ-ray spectra and luminosities on the pulsar period and magnetic field strength in a model where the γ-rays are produced by curvature radiation from primary particles. Data on the Crab and Vela pulsars were used to determine the primary particle energy and density, both of which put constraints on theories of particle acceleration in the magnetosphere. Using these parameters and the calculated spectra, we have determined how γ-ray luminosity scales with the quantities P and B for all other pulsars. A formula has also been derived for the γ-ray efficiency, which is found to increase with characteristic age as $\tau^{1.8}$.

General γ-ray luminosity formulae for pulsars have been derived by other authors. Cheng and Ruderman (1980) have estimated, from considerations of a large potential drop in the outer magnetosphere, that $L_\gamma \sim 5\times10^{30} B_{12} P^{-2}$ erg s^{-1} at several hundred MeV. Ayasli and Ögelman (1980) consider this outer gap model and calculate analytically the expected spectrum and luminosity. They conclude that $L_\gamma \propto P^{-1} B$ and that the γ-ray efficiency scales as $\tau^{3/2}$. These papers deal with a specific model of particle acceleration and include the effects of pair production only on the gap potential or in the form of a sharp energy cutoff. We have concentrated here on a detailed treatment of the pair production attenuation and its effects on the shape of the spectrum. The results are basically independent of the acceleration mechanism, given that γ_0 is no more than weakly dependent on pulsar parameters. While the derived dependence of the luminosity on these parameters is generally consistent with the previous derivations, the differences reflect the effects of pair production in the magnetosphere.

Future instruments aboard the proposed Gamma Ray Observatory (GRO) should be capable of detecting many more γ-ray pulsars. The number of observable sources in a disk population with surface density, N_0, at a given luminosity, L_0, is $N_s\ (> S_\gamma) = \frac{1}{8} L_0\ N_0/S_\gamma$, where S_γ is the γ-ray flux above 100 MeV. Assuming a mean pulsar period of 0.5 s. and magnetic field strength $B_0 = 10^{12}$ gauss, $L_0 \simeq 4\times10^{35}\ s^{-1}$. With a local pulsar surface density of $N_0 \simeq 500\ kpc^{-2}$ (Manchester 1979), $N_s\ (> S_\gamma) \simeq (1\times10^{-5}/S_\gamma)$ photons $s^{-1}cm^{-2}$. The number of observable sources which are pulsars should be of order 10 with the limiting sensitivity of COSB and 100 with GRO. The number which can be detected as pulsed γ-ray sources, however, is somewhat less, as only a fraction of these will have measured radio periods and period derivatives.

The author would like to thank D. J. Thompson, R. Ramaty, F. W. Stecker, and F. C. Jones for useful discussions and suggestions, and P. R. Backus for supplying data in advance of publication.

REFERENCES

Arons, J. and Scharlemann, E. T. 1979, Ap. J., 231, 854.

Ayasli, S. and Ögelman, H. 1980, Ap. J., 237, 227.

Bennett, K., Bignami, G. F., Boella, G., Buccheri, R., Hermsen, W., Kanbach, G., Lichti, G. G., Masnou, J. L., Mayer-Hasselwander, H. A., Paul, J. A., Scarsi, L., Swanenburg, B. N., Taylor, B. G. and Wills, R. D. 1977, Astron. Astrophys., 61, 279.

Buccheri, R., D'Amico, N., Massaro, E. and Scarsi, L. 1978, Nature, 274, 572.

Cheng, A. and Ruderman, M. 1980, preprint.

Cheng, A., Ruderman, M. A., and Sutherland, P. G. 1976, Ap. J., 203, 209.

Daugherty, J. K. and Lerche, I. 1975, Ap. Space Sci., 38, 437.

Harding, A. K., Tademaru, E. and Esposito, L. W. 1978, Ap. J., 225, 226 (Paper I).

Jackson, J. D. 1962, Classical Electrodynamics (New York: Wiley).

Kniffen, D. A., Hartman, R. C., Thompson, D. J., Bignami, G. F., Fichtel, C. E., Ögelman, H. and Tümer, T. 1974, Nature, 251, 397.

Lichti, G. G., Buccheri, R., Caraveo, P., Gerardi, G., Hermsen, W., Kanbach, G., Masnou, J. L., Mayer-Hasselwander, H. A., Paul, J. A., Swanenburg, B. N. and Wills, R. D. 1980, Non-Solar Gamma Rays (COSPAR), ed. R. Cowsik and R. D. Wills (New York: Pergamon).

Manchester, R. N. 1979, Aust. J. Phys., 32, 1.

Manchester, R. N. and Taylor, J. H. 1980, A. J., in press.

Newton, L. M., Manchester, R. N. and Cooke, D. J. 1980, preprint.

Ögelman, H., Fichtel, C. E., Kniffen, D. A., and Thompson, D. J. 1976, Ap. J., 209, 584.

Ostriker, J. P. and Gunn, J. E. 1969, Ap. J., 157, 1395.

REFERENCES (Cont'd.)

Rappaport, S. and Joss, P. C. 1979,

Ruderman, M. A. and Sutherland, P. G. 1975, Ap. J., 196, 51.

Salvati, M. and Massaro, E. 1968, Astron. Astrophys., 67, 55.

Scharlemann, E. T., Arons, J., and Fawley, W. M. 1978, Ap. J., 222, 297.

Sturrock, P. A. 1971, Ap. J., 164, 529.

Taylor, J. H., Fowler, L. A., and McCulloch, P. M. 1979, Nature, 277, 437.

Thompson, D. J., Fichtel, C. E., Kniffen, D. A. and Ögelman, H. 1975, Ap. J. (Letters), 200, L79.

Thompson, D. J., Fichtel, C. E., Kniffen, D. A., Lamb, R. C. and Ögelman, H. B. 1976, Astrophysical Letters, 17, 173.

FIGURE CAPTIONS

Figure 1--Calculated spectra above 100 MeV for a magnetic field of 10^{12} gauss, initial primary particle energy of 1×10^{7} and different values of the pulsar period in seconds.

Figure 2--Calculated spectra above 100 MeV for a magnetic field of 10^{12} gauss, initial primary particle energy of 3×10^{7} and different values of the pulsar period in seconds.

Figure 3--Calculated spectra above 100 MeV for a magnetic field of 5×10^{12} gauss, initial primary particle energy of 3×10^{7} and different values of the pulsar period in seconds.

Figure 4--Fits of calculated spectra to observed spectra of the Crab and Vela pulsars. Data points are from Lichti et al. 1980.

Figure 5--Gamma ray efficiency times the quantity $(\dot{P}_{crab}/\dot{P})^{1/3}$ plotted against characteristic age.

TABLE 1

PREDICTED PULSAR γ-RAY FLUXES (> 100 MeV)

PSR	P(s.)	$\dot{P}(10^{-15}$ s $s^{-1})$	d(kpc)	$B_o(10^{12}G)$	L_γ(photons s^{-1})	Φ_γ(photons s^{-1} cm^{-2})
0531+21	0.033200	421.996	2.0	3.8	1.39×10^{38}	3.65×10^{-6}
0655+64	0.195671	1.481*	0.14	0.54	9.77×10^{35}	5.2×10^{-6}
0656+14	0.384860	--	0.31	1.0	5.68×10^{35}	6.2×10^{-7}
0743-53	0.214837	2.73†	0.39	0.77	1.18×10^{36}	8.18×10^{-7}
0833-45	0.089243	124.268	0.50	3.4	2.32×10^{37}	9.73×10^{-6}
0922-52	0.746295	35.477†	0.45	5.21	9.59×10^{35}	4.97×10^{-7}
0950+08	0.253065	0.2321	0.10	0.2	2.32×10^{35}	2.43×10^{-6}
1133+16	1.187910	3.7322	0.18	2.1	1.76×10^{35}	5.69×10^{-7}
1552-31	0.518111	--	0.17	1.0	3.43×10^{35}	1.24×10^{-6}
1552-23	0.532576	--	0.15	1.0	3.27×10^{35}	1.53×10^{-6}
1600-27	0.778311	--	0.14	1.0	1.72×10^{35}	9.19×10^{-7}
1642-03	0.387689	1.7803	0.16	0.84	4.71×10^{35}	1.93×10^{-6}
1648-17	0.973388	3.031*	0.16	1.74	2.04×10^{35}	8.36×10^{-7}
1700-18	0.804340	--	0.18	1.0	1.62×10^{35}	5.26×10^{-7}
1702-18	0.298986	--	0.17	1.0	8.72×10^{35}	3.17×10^{-6}
1706-16	0.653050	6.369	0.16	2.1	4.85×10^{35}	1.99×10^{-6}
1747-46	0.742352	1.295†	0.74	0.99	1.84×10^{35}	3.53×10^{-8}
1929+10	0.226517	1.158	0.11	0.52	7.27×10^{35}	6.31×10^{-6}
2151-56	1.373653	4.23 †	0.18	2.44	1.59×10^{35}	5.16×10^{-7}

* P.R.Backus,private communication
† from Newton, Manchester and Cooke 1980

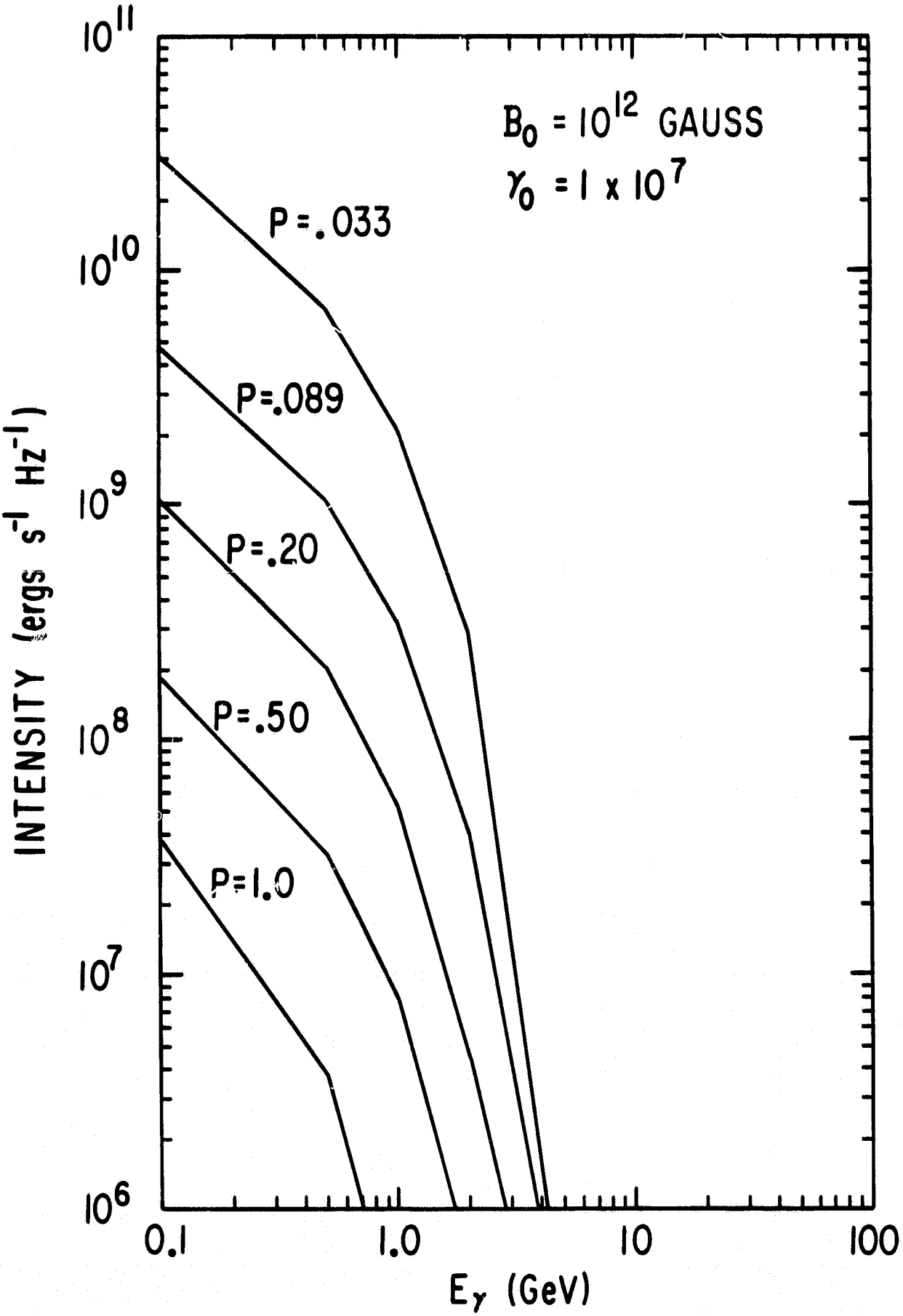
10^{11}
10^{10}
10^{9}
10^{8}
10^{7}
10^{6}
INTENSITY (ergs s^{-1} Hz^{-1})
$B_0 = 10^{12}$ GAUSS
$\gamma_0 = 1 \times 10^{7}$
P = .033
P = .089
P = .20
P = .50
P = 1.0
0.1
1.0
10
100
E_γ (GeV)

Figure 1

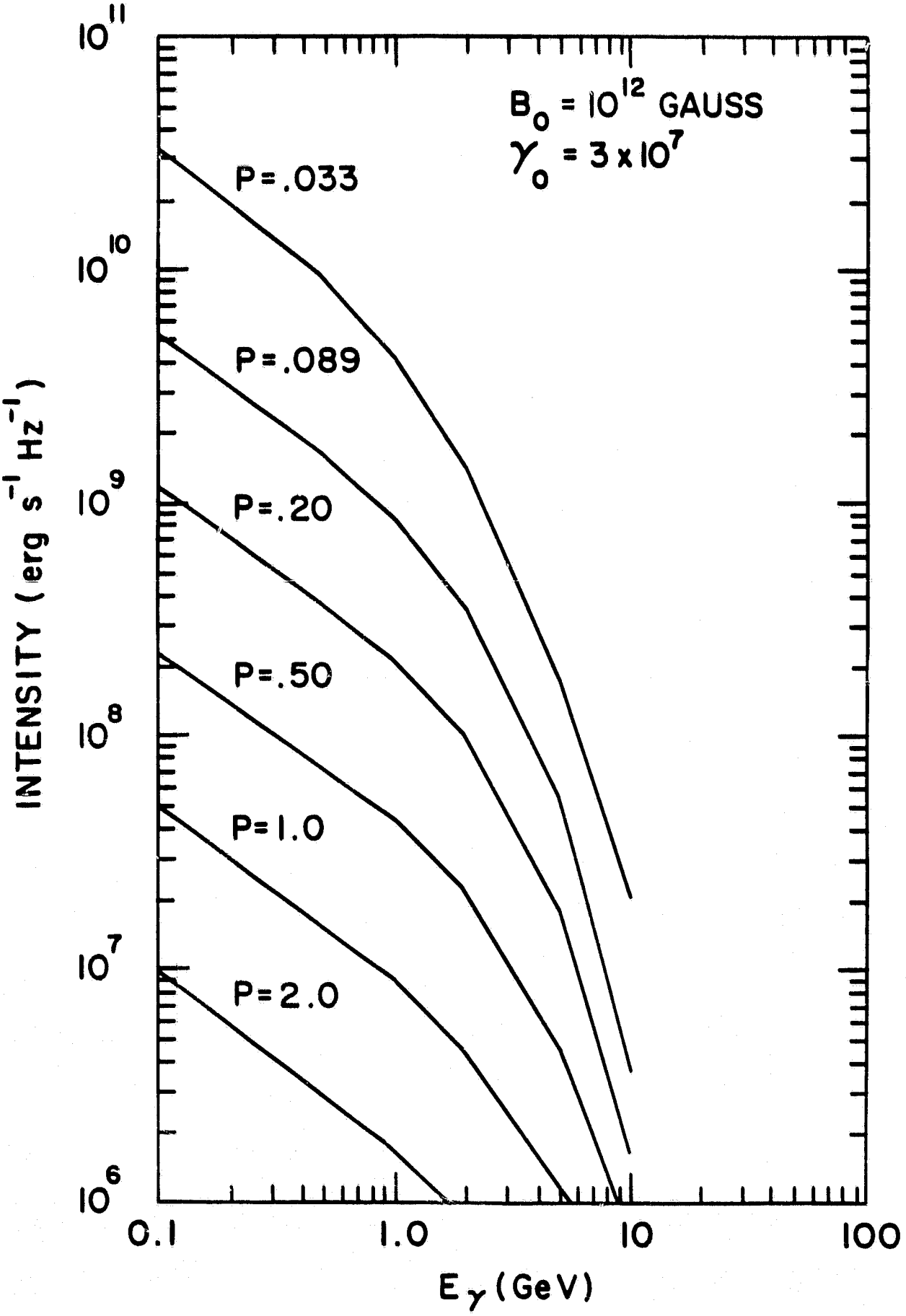
$B_0 = 10^{12}$ GAUSS
$\gamma_0 = 3 \times 10^7$
P=.033
P=.089
P=.20
P=.50
P=1.0
P=2.0
INTENSITY (erg s^{-1} Hz^{-1})
10^{11}
10^{10}
10^9
10^8
10^7
10^6
0.1
1.0
10
100
E_γ (GeV)

Figure 2

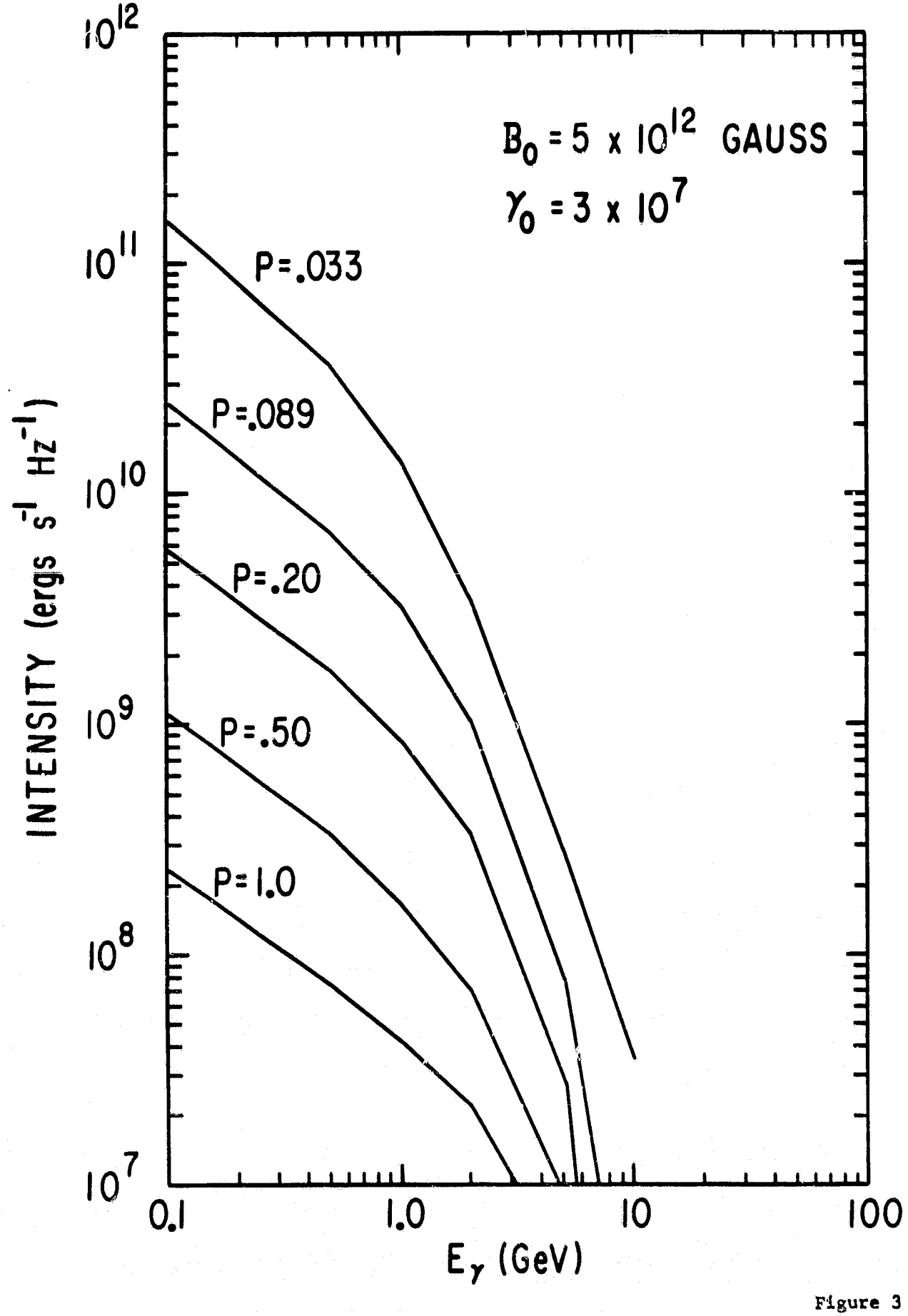
$B_0 = 5 \times 10^{12}$ GAUSS
$\gamma_0 = 3 \times 10^7$
P=.033
P=.089
P=.20
P=.50
P=1.0
INTENSITY (ergs s^{-1} Hz^{-1})
10^{12}
10^{11}
10^{10}
10^9
10^8
10^7
0.1
1.0
10
100
E_γ (GeV)

Figure 3

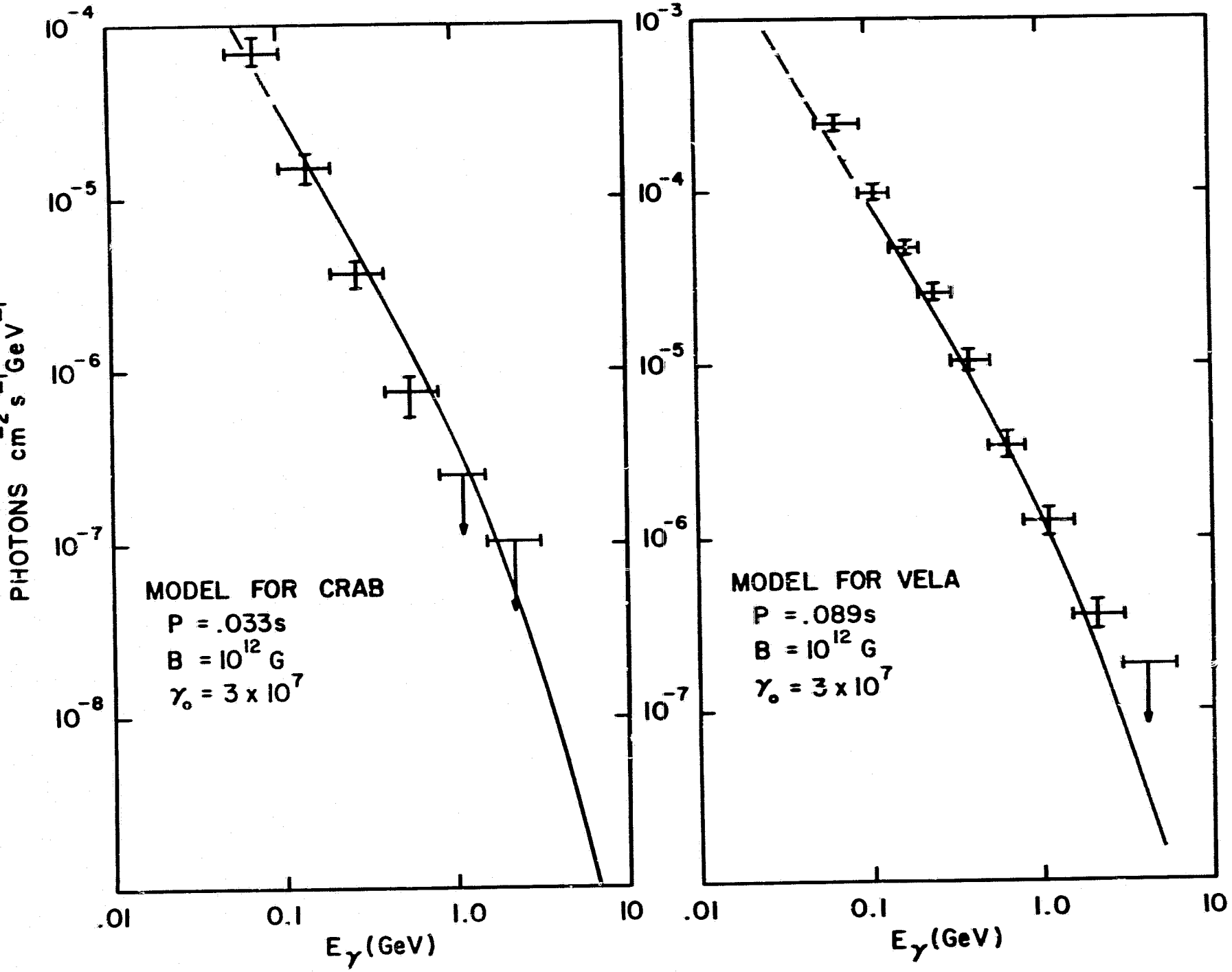
PHOTONS cm^{-2} s^{-1}GeV^{-1}
10^{-4}
10^{-5}
10^{-6}
10^{-7}
10^{-8}
MODEL FOR CRAB
P = .033s
B = 10^{12} G
γ_o = 3 x 10^7
.01
0.1
1.0
10
E_γ(GeV)
10^{-3}
10^{-4}
10^{-5}
10^{-6}
10^{-7}
MODEL FOR VELA
P = .089s
B = 10^{12} G
γ_o = 3 x 10^7
.01
0.1
1.0
10
E_γ(GeV)

Figure 4

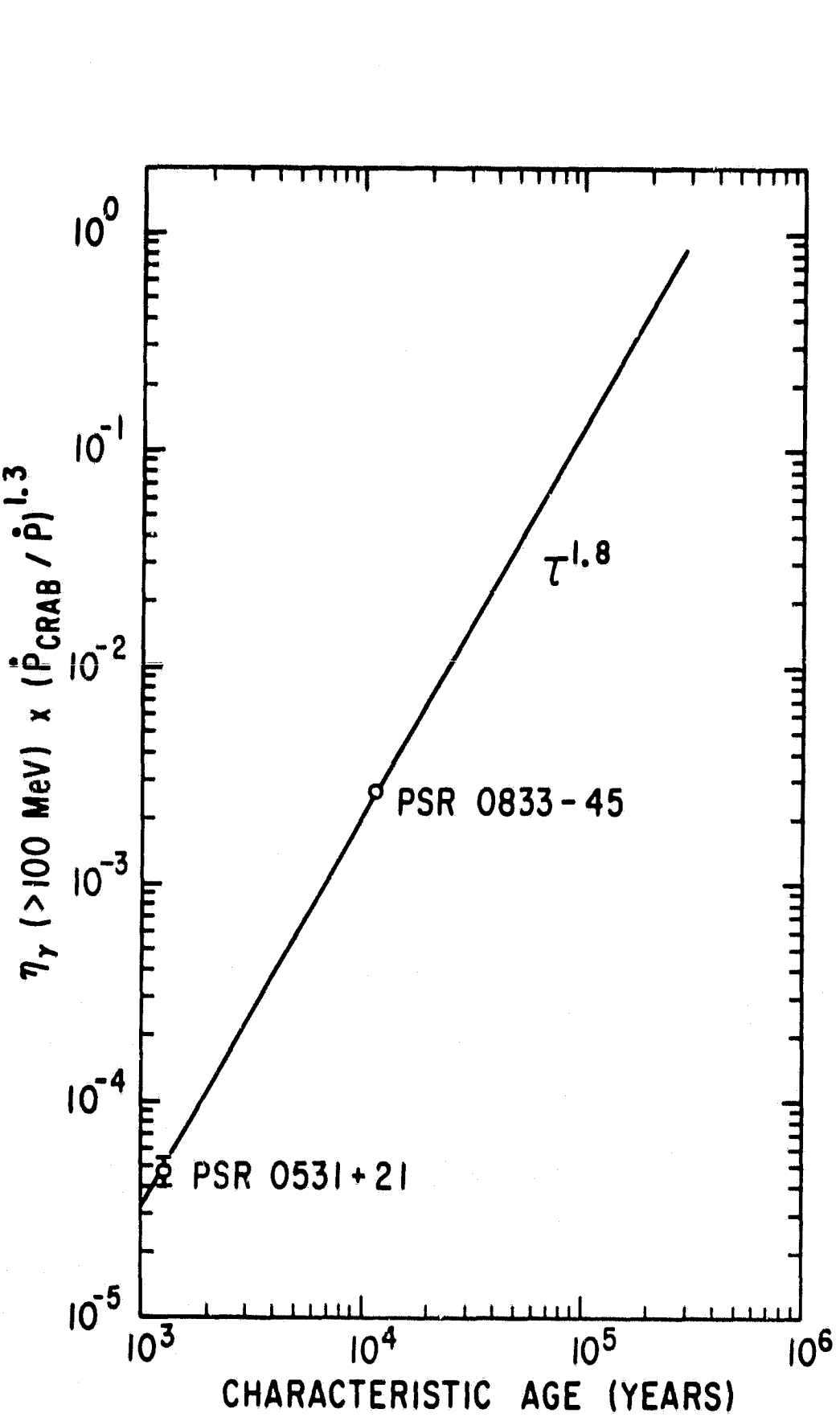
10^0
10^{-1}
10^{-2}
10^{-3}
10^{-4}
10^{-5}
η_γ (>100 MeV) x $(\dot{P}_{CRAB}/\dot{P})^{1.3}$
$\tau^{1.8}$
PSR 0833-45
PSR 0531+21
10^3
10^4
10^5
10^6
CHARACTERISTIC AGE (YEARS)

Figure 5